ELSEVIER

Journal of Nuclear Materials 258–263 (1998) 1158–1162

journal of nuclear materials

Solubility product and precipitation of TaC in Fe–8Cr–2W steel

M. Tamura [a,*], K. Shinozuka [a], K. Masamura [b], K. Ishizawa [c], S. Sugimoto [c]

[a] *Department of Materials Science, National Defense Academy, Hashirimizu, Yokosuka-shi 239, Japan*
[b] *NKK Co., Kawasaki-ku, Kawasaki-shi 210, Japan*
[c] *Kokan-Keisoku Co., Kawasaki-ku, Kawasaki-shi 210, Japan*

Abstract

The precipitation behavior of TaC in austenite was studied to improve mechanical properties of a reduced-activation steel, Type F-82H (an 8%Cr–2%W steel). The solubility product of TaC in austenite of Type F-82H was determined as a function of temperature and was 70% larger than that of γ-Fe. On metallurgical examination, the following was found: (1) The nucleation and growth of austenite grains and/or the reverse $\alpha \rightarrow \gamma$ transformation accelerated the precipitation of fine particles of TaC, and the fine precipitates suppressed the further growth of the austenite grains. (2) When homogenizing at 1523 K previously, coarse austenitic grains were observed by heating at 1223–1323 K as compared with the grains after directly heating of the hot-rolled plate, while the solubility product itself was roughly independent of the homogenizing treatment.

1. Introduction

Recently developed reduced-activation ferritic steels contain a small amount of Ta. It was reported that Ta increased both rupture strength and toughness when a suitable heat treatment was applied [1,2], and excess addition of Ta decreased toughness in the weld metal [3]. However, the basic and systematic investigation on the role of Ta has not yet been presented. The solubility product equations of TaC and TaN in γ-Fe has been reported [4], but the Ta contents of the specimens used were one order and more of magnitude higher than those of the steels of interest and, moreover, the effects of Cr and W on the solubility product were not clarified. In the present study, the precipitation behavior of TaC and the solubility product in austenite of a reduced-activation ferritic steel, Type F-82H, which is the prime candidate structural material of the blanket and the first wall of a steady state tokamak reactor [5], have been investigated.

2. Experimental procedure

Three experimental alloys with different Ta contents were melted in a 50 kg induction furnace. The chemical compositions are given in Table 1. The ingots were hot-rolled to 12 mm thickness, where the final pass was made at 1173 K for each. Coupons were cut from the hot-rolled plates and aged at temperatures from 1223 up to 1523 K for 1.8 to 324 ks followed by air cooling. Some coupons were homogenized at 1523 K for 1.8 ks before the aging. Precipitated phases were extracted using a 10% acetyl acetone/1% tetramethyl ammonium chloride/methanol electolyte, and the Ta contents in the extracted residues were analyzed precisely by an inductively coupled plasma atomic emission spectroscope. The morphology and composition of the extracted phases were investigated under a scanning electron microscope (SEM) and a transmission electron microscope (TEM). The crystal structures of the extracted phases and the austenitic grain sizes measured by the comparison method were also investigated.

3. Results and discussion

3.1. Solubility product

Narita et al. [4] reported the solubility product equation of TaC where Ta and C contents in austenite were calculated as the difference of the total Ta and C

* Corresponding author. E-mail: mtamura@cc.nda.ac.jp.

0022-3115/98/$19.00
PII: S0022-3115(98)00151-2

Table 1
Chemical composition (mass%)

Alloy	C	Si	Mn	P	S	Cr	W	V	Ta	Ti	N	Al	Fe
A	0.096	0.11	0.49	0.0012	0.0032	7.83	1.91	0.19	0.046	0.008	0.0088	0.017	Bal.
B	0.097	0.11	0.49	0.0010	0.0033	8.08	1.96	0.20	0.109	0.005	0.0099	0.020	Bal.
C	0.079	0.11	0.48	0.0006	0.0034	7.99	1.96	0.19	0.206	0.005	0.0023	0.019	Bal.

contents and those of the residues. However, this method is not always suitable, because the accuracy of carbon analysis in an extracted residue is generally not so high. In this study, the solubility product of TaC was determined based on the following assumptions: (1) the composition of TaC is stoichiometric, which means that the solubility product is determined from the precisely analyzed Ta contents so that analysing C in the residue is not necessary, (2) dissolution of N in TaC is neglected, because the total nitrogen contents in the alloys are very low and (3) Ta in inclusions is also neglected.

Table 2 shows the conditions of the heat treatments and the Ta contents in the extracted residues. The word called aging of the 4th and 5th columns in Table 2 is used aiming at the precipitation of TaC, though this treatment is usually called normalizing. The second aging treatment showed in Table 2 is explained later. The solubility products of TaC were calculated using the Ta contents, and the results are plotted in Fig. 1 as a function of inverse absolute temperature. In the figure, the data of No. 4, 15, 21 and 22 were omitted for simplicity, because the solubility products were near each product of the total Ta and C contents, i.e. almost all of the Ta and C dissolved into the matrix independent of the aging temperature.

It was found from Table 2 that when the aging temperature was high enough, undissolved Ta in Alloys A and B became very low, but in Alloy C the undissolved Ta-compounds were still present. In specimen No. 22, the Ta content in the residue was rather high, as compared with specimens No. 20 and 21, which corresponded to both the presence of a small amount of

Table 2
Tantalum contents in the extracted residues of the aged specimens and related properties

No.	Alloy	Homogenizing temperature (K × 1.8 ks)	Aging temperature (K)	Aging time (ks)	Second aging temperature (K × 1.8 ks)	Ta in residue (%)	Vickers hardness No. HV10	Austenite grain size No.	X-ray diffraction
1	A		(as rolled)			0.005	389		
2	A		1223	1.8		0.027	395	8	TaC, Unknown
3	A	1523	1223	1.8		0.022	392	4 [a]	
4	A	1523	1323	1.8		0.005	382	5	
5	A	1523	1323	1.8	1223	0.014	379	6	
6	B		(as rolled)			0.005	390		
7	B		1223	1.8		0.08	391	8.5	
8	B		1223	21.6		0.073	389		
9	B		1273	1.8		0.067	390	8	
10	B		1323	21.6		0.017	382		
11	B		1323	324		0.039	333		
12	B	1523	1223	1.8		0.079	391	3 [a]	
13	B	1523	1273	1.8		0.057	389	4.5 [a]	
14	B	1523	1373	1.8		0.008	384	5	
15	B	1523	1473	1.8		0.005	382	3.5	
16	B	1523	1473	1.8	1223	0.022	382	4.5	
17	B	1523	1473	1.8	1323	0.019	384	4	
18	C	1523	1323	1.8		0.086	373	6.5 [a]	TaC, Unknown
19	C	1523	1373	1.8		0.048	378	6.5	
20	C	1523	1423	1.8		0.023	373	6	
21	C	1523	1473	1.8		0.021	372	5	
22	C	1523	1523	1.8		0.033	361	5 [b]	Unknown

[a] Non-uniform grain size.
[b] with small amount of δ-ferrite.

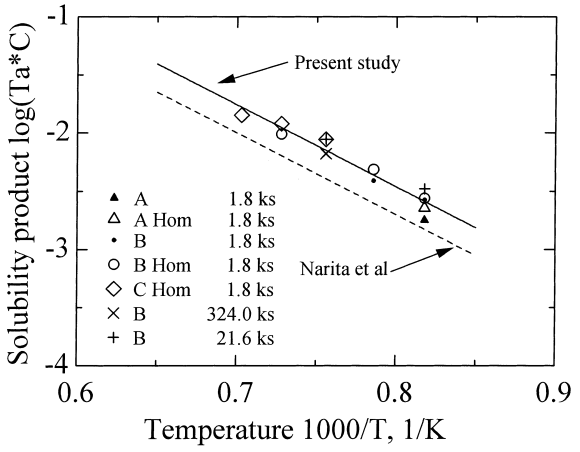

Fig. 1. Relation between solubility product of TaC in austenite and aging temperature. The explanations for symbols mean the name of alloy, the enforcing of homogenization and the aging time, respectively.

δ-ferrite and the rather low Vickers hardness number. This may suggest the precipitation of TaC in δ-ferrite or at the boundaries between δ and γ.

In Fig. 1, the data of the longer aging time than 1.8 ks or without homogenizing treatment were distinguished from the others. However, the figure shows that the data for specimens without a homogenizing treatment fall in the scatter band of those with a homogenizing treatment. The figure also shows that the solubility products did not vary much even if the aging time was changed in a wide range of 1.8–324 ks. Therefore, the regression analysis was made on all the data plotted in the figure, and the following solubility product equation was obtained with high correlative coefficient of $R = 96\%$:

$$\log([\%\mathrm{Ta}]_\gamma[\%\mathrm{C}]_\gamma) = -7027/T + 3.16, \quad (1)$$

where T was aging temperature in K, % is mass%. It was found that the solubility product of TaC in austenite of an Fe–Cr–W alloy was about 70% larger than that of γ-Fe [4] through a wide range of the aging temperature.

The X-ray diffraction analyses on the extracted residues of the aged alloys showed two weak peaks with interplaner spacings of 0.21 and 0.25 nm beside the main peaks for TaC. It was difficult to identify these unknown peaks, but they resemble those of Al_2O_3. Three types of inclusions were observed in SEM, and an energy dispersive X-ray spectrometer (EDS) showed that most of the inclusions were probably Al_2O_3 and, besides these, the main components of a few inclusions were Si and Ti. The inclusions of a TiN type were rectangular and about 0.2 μm. They contained a small amount of Ta and S in some cases. When aging temperature was high enough to dissolve most of the Ta into the matrix, the Ta contents in the residues were less than 10% of the total Ta contents of the alloys, as shown in Table 2. Therefore, the 3rd assumption mentioned above was reasonable.

The direct observation of the aged specimens in a field emission SEM-EDS showed that the main elements in the precipitates were Ta and C, but the weak peaks of Fe, Cr and Ti were from the precipitates. The peaks of Fe and Cr might come from the matrix and the Ti from the precipitates. The back scattered electron images showed a uniform and bright contrast at the precipitates, so that the detected Ti might be dissolved in the precipitates. In any case, the total Ti contents were negligibly small and the behavior of Ti was neglected.

The present analysis was based on stoichiometry of TaC, but the binary phase diagram of Ta and C suggests that the ratio of C/Ta of TaC is in the range from 0.7 to 1 and is probably less than one. Therefore, the above solubility product equation included some error based on the non-stoichiometric compositional ratio of TaC. However, the possible error in the above solubility product equation should be less than 5% no matter how large it was. The reason is as follows: the ratio of the approximate value to the true solubility product is roughly equal to $[1 - C_p/C_t(1-\alpha)]$ when $C_p/C_t < 1$, where $\alpha = \mathrm{C/Ta}$ in an actual carbide and C_p and C_t are the assumed carbon contents in a stoichiometric TaC precipitate and the carbon contents in the total, respectively. In the present study, C_p/C_t is estimated to be less than 0.072 from Table 2: $C_p = (\%\mathrm{Ta}\text{ in the residue})/180.95 * 12$ and the maximum value of C_p/C_t is $0.086/180.95 * 12/0.079 = 0.072$ for specimen No. 18. Namely, the true solubility product should be only about 2% or less larger than that of Eq. (1), even though $\alpha = 0.7$, which corresponds to the minimum carbon value in the phase diagram.

When a precipitate is small, the equilibrium solubility increases according to the theory by Wagner [6], and thus the solubility product increases. Akamatsu et al. [7] reported that this effect was negligibly small in a similar system, Fe–C–Nb, when C/Nb > 1, so that the effect should be also negligible in this case, an Fe–C–Cr–W–Ta system.

3.2. Precipitation of TaC

Fig. 1 showed that the total amount of TaC precipitated was not roughly affected by the homogenizing treatment at 1523 K prior to the aging treatment. However, Table 2 shows that the homogenizing made the prior austenite grain coarse and non-uniform (see No. 3, 12, 13, 18) when aged at rather low temperatures, i.e. 1223–1323 K. Table 2 also shows that if the aging temperature was raised beyond this temperature range, the Ta contents in the residues decreased abruptly, and rather small and uniform grains were observed (see No. 4, 14, 15, 19, 20, 21).

On the contrary, when the second aging treatment was made subsequent to the first aging (for example, in the case of No. 16) after holding at the first aging temperature (1473 K for 1.8 ks) and then cooling directly to the second aging temperature at 1223 K without cooling down to room temperature, and then aging for 1.8 ks followed by air cooling, only a little Ta was observed in the residue, as compared with directly aging at 1223 K (compare No. 5 with No. 2 or No. 3 and No. 16 with No. 7 or No. 12 in Table 2). In this case, the austenite grains were coarsened by the first aging as listed in Table 2.

Fig. 2 shows the morphology of TaC particles in the extracted replicas of Alloy B with the different heat treatments. In the directly aged specimen of the hot-rolled plate without both the homogenizing treatment and the second aging treatment (No. 7), very fine particles of about 10 nm were distributed uniformly in a high density in the grains, and rather coarse particles of about 10–60 nm were precipitated at the boundaries, as shown in Fig. 2(a). The main components of most of the precipitates investigated by TEM were Ta and C. Vanadium and Ti were also found in some cases as minor elements. The similar morphology was also observed, as shown in Fig. 2(b) in the homogenized and then aged specimen (No. 12). On the other hand, in the second aged specimen (No. 16) fine TaC particles of about 10 nm were hardly found and a few particles of several tens of nanometers were found (Fig. 2(c)). These were thought to be the undissolved compound, TaC and TiN. In some cases TaC was precipitated on a rectangular TiN particle.

It is generally questionable to discuss quantitatively the distribution and/or the amount of precipitates using a replica. But the SEM observations were consistent with the Ta contents in the residues, as shown in Table 2. Therefore, the microstructures of Fig. 2 are considered to show the characteristics of the precipitation behavior of TaC.

The second aging treatment might be seen as a special case because it is a little complex. However, this is a general treatment, i.e. solid-solutioning followed by aging without any accompanying transformation. Therefore, the nucleation and growth mechanism should be mainly controlling the precipitation behavior [8]. Namely, heterogenous nucleation sites were limited in the fully recrystallized austenite so that the homogeneous nucleation and growth mechanism became the main precipitation process, and the second aging time of 1.8 ks was not sufficient to precipitate fully. This is reasonable based on results from the literature for similar alloy systems: in the case of Nb-bearing ultra low carbon steel, it took several hours to saturate the precipitation of NbC in a similar treatment as the second aging [9] and, in case of a high strength low alloy steel, it also took several hours for the 50% Nb(C,N) precipitation when the applied strain in an austenitic state was 1% [10].

On the other hand, the precipitation rate observed in the directly aged specimen (No. 7) was very high. It is surprising that aging for 1.8 ks was enough to saturate the precipitation of TaC without any high-temperature deformation to provide the nucleation sites. Therefore,

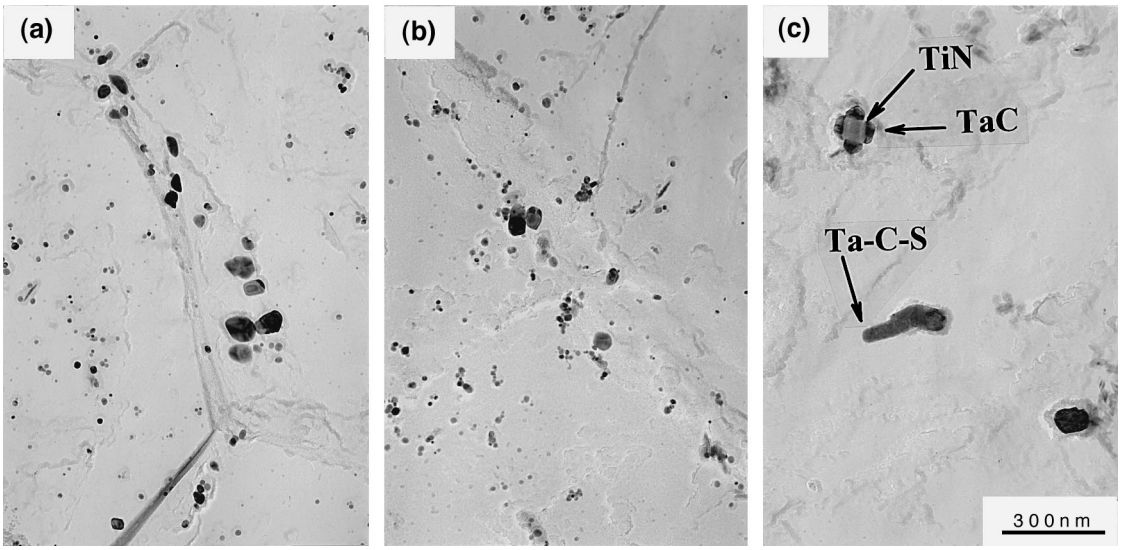

Fig. 2. TEM images of the extracted replicas of Alloy B: (a) aged at 1223 K (No. 7), (b) homogenized at 1523 K and then aged at 1223 K (No. 12) and (c) homogenized at 1523 K and then intermediately aged at 1473 K followed by aging at 1223 K (No. 16). Fig. 2(a) and (b) show the TaC particles precipitated intergranularly and intragranularly and Fig. 2(c) shows the TaC precipitated on a rectangular TiN particle and a complex compound of the Ta–C–S system.

the precipitation in specimen No. 7 should be much accelerated by some factors relating to the $\alpha \rightarrow \gamma$ transformation. The details of the $\alpha \rightarrow \gamma$ transformation are not yet clear, but usually the heterogeneous nucleation of austenite may occur at the prior austenite boundaries in an as-rolled state [11–14]. Immediately after the transformation many nucleation sites might exist and a lot of nuclei of TaC should be rapidly precipitated from the supersaturated austenite, and the precipitates disturb the grain growth as long as the precipitates are thermodynamically stable.

As shown in Table 2, the non-uniform and large austenite grains were observed when the homogenizing treatment was applied prior to the aging treatment. In this case, beside the nucleation and growth mechanism the reverse $\alpha \rightarrow \gamma$ transformation of martensite to austenite should also operate. This transformation may occur martensitically, and many defects are left in the austenite. The defects may induce the local recrystallization of the newly transformed austenite [15] as well as the defects themselves acting as the nucleation sites. According to this rapid transformation, the expeditious precipitation of TaC may occur as shown in Table 2 and Fig. 2(b), where the Ta content in the residue of No. 12 was comparable to that of the directly aged specimen, i.e. No. 7.

4. Conclusion

The precipitation behavior of TaC in a reduced-activation ferritic steel, Type F-82H, was studied and the following conclusions were obtained.

1. The solubility product of TaC in austenite of an 8%Cr–2%W steel was determined (Eq. (1) in the text). It was found to be 70% larger than that in γ-Fe.
2. Finely dispersed TaC particles were observed in a high density by aging at temperatures just above the $\alpha \rightarrow \gamma$ transformation for a relatively short time.
3. The reverse $\alpha \rightarrow \gamma$ transformation and/or the nucleation and growth of austenitic grains accelerated the precipitation of the fine particles of TaC, and the fine precipitates suppressed the further growth of the austenitic grains.
4. When a homogenizing treatment at 1523 K was applied prior to the precipitation treatment, coarse austenitic grains were observed after the precipitation treatment, while the solubility product itself was roughly independent of the homogenizing treatment.

References

[1] M. Tamura, H. Hayakawa, M. Tanimura, A. Hishinuma, T. Kondo, J. Nucl. Mater. 141–143 (1986) 1067.
[2] M. Tamura, H. Hayakawa, A. Yoshitake, A. Hishinuma, T. Kondo, J. Nucl. Mater. 155–157 (1988) 620.
[3] H. Hayakawa, A. Yoshitake, M. Tamura, S. Natsume, A. Gotoh, A. Hishinuma, J. Nucl. Mater. 179–181 (1991) 693.
[4] K. Narita, S. Koyama, Kobe Steel Engineering Reports 16 (1966) 179.
[5] Y. Seki, SSTR Design team, 13th International Conference On Plasma Phys. and Contr. Nucl. Fusion Res., IAEA-CN-53/G-1-2, 1990.
[6] R.A. Oriani, Acta Met. 12 (1964) 1399.
[7] S. Akamatsu, T. Senuma, M. Hasebe, J. Iron Steel Inst. Jpn. 78 (1992) 790.
[8] For example, L.H. Van Vlack, Elements of Materials Science and Engineering, 6th ed., Addison-Wesley, Reading, MA, 1990, p. 223.
[9] S. Akamatsu, Y. Muramatsu, T. Senuma, H. Yada, S. Ishikawa, J. Iron Steel Inst. Jpn. 75 (1989) 933.
[10] B. Dutta, C.M. Sellars, Mater. Sci. Technol. 3 (1987) 197.
[11] M. Maki, H. Morimoto, I. Tamura, J. Iron Steel Inst. Jpn. 65 (1979) 1598.
[12] K. Nakazawa, Y. Kawabe, S. Muneki, J. Iron Steel Inst. Jpn. 67 (1981) 1795.
[13] T. Utsunomiya, K. Hoshino, T. Sakuma, H. Suto, J. Iron Steel Inst. Jpn. 73 (1987) 1582.
[14] M. Murata, K. Nishioka, H. Tamehiro, J. Iron Steel Inst. Jpn. 74 (1988) 1454.
[15] S. Matsuda, Y. Okamura, J. Iron Steel Inst. Jpn. 60 (1974) 226.